

MATHEMATICAL MODELING OF THE PASSAGE OF THE NUCLEONIC-NUCLEAR COMPONENT OF COSMIC RADIATION THROUGH THE EARTH'S ATMOSPHERE

G. V. Miloshevskii and G. S. Romanov

UDC 539.1

A theoretical model is worked out and a characteristic is given for the physical processes occurring in the passage of high-energy neutrons and protons through the earth's atmosphere. A mathematical model of internuclear and intranuclear cascades is presented. The process of nuclear spallation is regarded as consisting of direct expulsion of one or several high-energy nucleons from a nucleus and de-excitation of the residual nucleus in the form of an evaporation cascade. The mathematical model is based on the Monte Carlo method. Results of numerically modeling the passage of the proton component through an actual atmosphere are presented.

Introduction. Studying the passage of cosmic radiation through the atmosphere is of great importance for two reasons. First, cosmic-ray particles set up additional ionization in the earth's ionosphere (region *D*), thus causing interference with radio communication in various radio-frequency ranges, especially at night. Therefore, modeling the rate of formation of ions by cosmic radiation in relation to its intensity and energy spectrum is of interest for predicting the state of the ionosphere in its lower part. Second, cosmic radiation (mainly secondary, resulting from nuclear reactions) reaches the earth's surface and produces irradiation of living organisms. It is established that the sources of galactic rays are supernovas and their remains. With a supernova outburst, the flux of hard radiation of very high intensity can exceed the normal level by tens and hundreds of times. Therefore, numerical modeling of the radiation background on the earth's surface in relation to the intensity and energy spectrum of the primary particles is of high priority.

A major portion of the cosmic-ray particles falling on the boundary of the atmosphere are of galactic origin. Over 90% of the primary-radiation particles are protons. Penetrating into the atmosphere, they initiate a variety of interactions that persist over many successive generations and give rise to a host of particles. All these particles form secondary electron-photon and meson components. To describe adequately the development of particle cascades in the atmosphere, consideration should be given foremost to the behavior of the nucleonic component. Similarly to the electron-photon component, nucleons multiply in the atmosphere by a cascade process. However, in the case of nucleons it is necessary to take into account internuclear and intranuclear cascades.

1. Physical Model and Processes of Interaction of Nucleons with Nuclei. The physical model describing the passage of high-energy nucleons through the earth's atmosphere is based on the familiar approximation of binary collisions [1]. Here a nucleon is assumed to interact simultaneously with just one nucleus. For the phenomenon in question this approximation is justified, since the density of the incident flux of cosmic radiation is low. The interaction process is viewed as spatially localized. Then, the nucleon trajectory can be constructed in the form of a broken line connecting the points of successive collisions. At the points of interaction elastic scattering or a nuclear reaction occurs, and the states of the nucleon and the nucleus change. The probability of various processes (scattering, capture, or nuclear reaction) is determined by the macroscopic cross sections.

We now consider the elementary processes of interaction of protons and neutrons that have an energy of 1 keV or more with atmospheric nuclei. A decisive role in decelerating high-energy protons is played by the

Academic Scientific Complex "A. V. Luikov Heat and Mass Transfer Institute," National Academy of Sciences of Belarus, Minsk, Belarus. Translated from *Inzhenerno-Fizicheskii Zhurnal*, Vol. 72, No. 6, pp. 1121-1128, November-December, 1999. Original article submitted April 14, 1999.

processes of elastic scattering from nuclei and electrons, excitation and ionization of atmospheric nuclei, nuclear reactions, and nuclear excitation. We will briefly discuss elastic scattering and ionization loss. The cross section of elastic scattering of a proton on a nucleus was found in the first Born approximation by the Rutherford law [2]. It follows from the latter that there is a large probability of small-angle scattering. A large-angle deviation is a fairly rare event. Therefore, all interactions of a proton were divided into two groups, namely, strong with an angle of deviation $\theta > \theta^*$ and weak with $\theta < \theta^*$. Deviations by angles $\theta > \theta^*$ were regarded as individual events and deviations by the angles $\theta < \theta^*$ on a certain trajectory length L were taken into account on the basis of multiple-scattering theory [3]. According to this theory, account for small angles consists in that the proton direction at the end of the length L deviates by an angle found from the Gauss distribution [4]. The loss of the energy of protons is caused by ionization and excitation of the electron shells of atmospheric atoms. The cross section of transfer of energy to an atomic electron [2] was also obtained in the Born approximation. This cross section is very large when low energy is transferred. Therefore, all collisions of protons with electrons were subdivided into two groups, namely, near collisions with energy transfer $\Delta T > T^*$ and distant collisions with $\Delta T < T^*$. The former were treated as individual events, and the latter were taken into account in the approximation of continuous deceleration [2].

Let us consider in more detail the nuclear interactions of protons and neutrons (nucleons) with atmospheric nuclei. The nuclear reactions of protons start to compete with the above-mentioned processes at energies of 100 MeV. The elastic and inelastic nuclear interactions between neutrons and atmospheric nuclei are the main processes. The total microscopic cross section σ_t of nucleon-nucleus interaction is made up of the elastic scattering cross section σ_s and the reaction cross section σ_r , $\sigma_t = \sigma_s + \sigma_r$. The cross section σ_r includes all processes in which the state of the final nucleus is different from the state of the parent nucleus. The main difficulty in describing nuclear interactions of nucleons with matter is determining the cross sections. An accurate theoretical calculation of these cross sections should rely on knowledge of the forces acting between the nucleons in a nucleus. However, the properties of nuclear forces have been studied insufficiently as yet, and at present there is no theory that would allow a calculation of cross sections based on theoretical reasoning. All existing theoretical calculational methods basically have a phenomenological character and contain parameters selected from comparison with experiment. Therefore, cross sections of nuclear interactions of nucleons were calculated on the basis of an optical model [5, 6]. In this model, numerous interactions between individual nucleons are replaced by a two-body interaction of a nucleon and a nucleus as a unified whole described with the aid of a complex potential of appropriate form. This potential contains parameters selected from comparison with experiment and characterizing the distribution of intranuclear matter.

The total cross section of elastic scattering σ_s of a nucleon on a nucleus can be represented as [7]

$$\sigma_s = \frac{\pi}{k^2} \sum_{l=0}^{\infty} [(l+1) |1 - S_{l+1/2}|^2 + l |1 - S_{l-1/2}|^2].$$

The elements of the scattering matrix $S_{l\pm 1/2}$ were determined by solving the Schrödinger equation with the Woods-Saxon complex optical potential [8], whose real part describes elastic scattering and imaginary part describes absorption. Proton-nuclear cross sections in this potential should be calculated with allowance for the Coulomb interaction of the proton and the nucleus. The differential cross section of elastic scattering was calculated by the following equation [7]:

$$\begin{aligned} \frac{d\sigma_s}{d\Omega} = \frac{\pi}{k^2} & \left\{ \left| \sum_l \frac{1}{\sqrt{2l+1}} [(l+1)(1 - S_{l+1/2}) + l(1 - S_{l-1/2})] Y_l(\theta) \right|^2 + \right. \\ & \left. + \left| \sum_l \frac{1}{\sqrt{2l+1}} [(1 - S_{l+1/2}) + (1 - S_{l-1/2})] \frac{dY_l}{d\theta} \right|^2 \right\}. \end{aligned}$$

The cross section of inelastic processes σ_r was computed using the expression [7]

$$\sigma_r = \frac{\pi}{k^2} \sum_{l=0}^{\infty} [(l+1)(1 - |S_{l+1/2}|^2) + l(1 - |S_{l-1/2}|^2)].$$

With a low nucleonic energy, the main inelastic process is absorption followed by emission of nucleons or photons. With increase in the energy, as the reaction thresholds are overcome, the number of other inelastic channels grows.

2. Mathematical Models of Internuclear, Intranuclear, and Evaporation Cascades. The mathematical model of an internuclear cascade is based on direct modeling of the physical processes of interaction of nucleons with atmospheric atoms by the Monte Carlo method [9]. The interaction is described using macroscopic cross sections that characterize the probability of each of the processes considered. Neutron trajectories were simulated via a model of individual collisions [10] that successively treats all collisions experienced by a neutron. A model of grouping of small energy transfers [11] was used to simulate proton trajectories. After a proton traverses a certain trajectory length L particle characteristics in this model are determined from the distributions defining multiple scattering. The proton trajectory is constructed in the form of a broken line. On each of its segment a large number of weak collisions with a small energy loss and scattering angle occur. This can be accomplished considering that the interaction of charged particles is described by the Rutherford law and is associated with small scattering angles and small energy transfers. Therefore, it is possible to distinguish an average direction of the proton motion and thus fix the length L . At the end of the length L , a catastrophic collision occurs that is accompanied by a marked change in the energy or the scattering angle. Catastrophic collisions are treated as individual events.

In our model, nuclear spallation caused by a high-energy nucleon is regarded as consisting of two stages. In the first stage, the interaction of an incident nucleon with a nucleus is viewed as a set of individual statistically independent intranuclear collisions. The intranuclear cascade [12] was modeled on the basis of the Monte Carlo method. A nucleus was assumed to represent a degenerate Fermi gas of free nucleons enclosed in a spherical potential well with a radius equal to the nuclear. A nucleus is broken up by concentric spheres into several individual zones in each of which the nucleonic density and the potential are taken to be constant. By increasing the number of zones it is possible to approximate very accurately the initial distribution of the nuclear density and the potential. The case of motion of a nucleon within a nucleus is more complex than the motion in a homogeneous medium. The nuclear density is a function of the radius and, furthermore, the motion of the nuclei in the nucleus should be taken into account. As a consequence, the total cross section of nuclear interaction σ_t depends not only on the kind but also on the relative velocity of the colliding particles. The Pauli principle should also be taken into account. Since intranuclear nucleons occupy all energy levels up to the Fermi energy T_F , elastic interactions as a result of which a secondary nucleon will have an energy $T_N < T_F$ are excluded. The interaction can occur only on condition that a secondary nucleon has a kinetic energy $T_N > T_F$. Only in this case are the characteristics of a secondary nucleon memorized, and thereafter its history is traced similarly to a primary particle. No cascade nucleons with a kinetic energy ranging within $T_F < T < T_F + \varepsilon + T_b$ can escape from the nucleus. In the case of a proton, the Coulomb potential should be added to the right-hand side of this inequality. The magnitude of T_b is assumed to be of the order of or lower than the Coulomb energy. The choice of the energy T_b affects the boundary of cascade and evaporation particles. Once the history of an incident particle is completed and this particle has escaped from the nucleus or has been absorbed, we trace the histories of secondary nucleons resulting from the intranuclear interaction. The calculation is carried out until all cascade nucleons are absorbed or escape from the nucleus.

The intranuclear cascade yields a nucleus with an excitation energy E^* resulting from the fact that some fast nucleons did not manage to escape from the nucleus. The excitation energy of the residual nucleus is defined by the expression $E^* = T - E - (W - U)$. This energy is removed via emission of particles through the evaporation cascade [13]. In most cases neutrons, protons, α particles, and γ quanta are emitted. Their mean energy is of the order of 10 MeV. The number and energy distribution of these particles depend on the amount of energy that is left in the nucleus after the first stage of interaction is completed. The description of the evaporation cascade includes determination of the number and type of particles emitted by the nucleus, their angular and energy distributions, and mass and charge distributions of residual nuclei. Proceeding from the statistical character of the phenomenon, the evaporation cascade is considered with the aid of a Monte Carlo method that allows direct modeling of all specific features of the evaporation process.

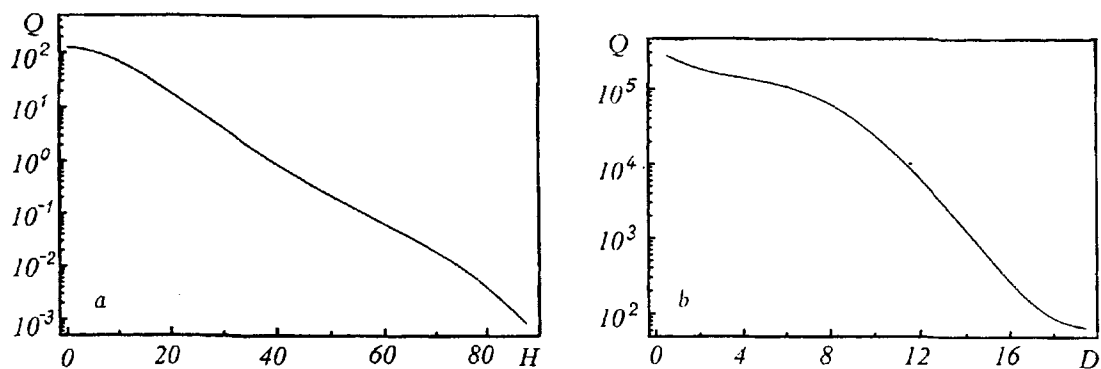


Fig. 1. Distribution of the rate of ion formation Q created by cosmic radiation over the atmospheric height (a) and over the earth's depth (b). Q , ion/(cm³·sec); H , km; D , m.

Formation of secondary particles (recoil nuclei, electrons, positrons, photons, and products of nuclear reactions) at points of collision leads to branching of trajectories. The trajectories of the primary and all secondary particles are traced as long as their energies are higher than the threshold energy or until they are absorbed. Passage of electrons, photons, and positrons through the atmosphere was modeled using a theoretical model [14]. Modeling of a single history is assumed to be completed if all trajectory branches have been constructed. The results of final sampling from N histories thus obtained are subsequently processed using statistical methods.

3. Results of Numerical Modeling. Based on the foregoing theoretical model, numerical modeling was performed for passage of the proton component of cosmic radiation through the earth's atmosphere with allowance for its actual characteristics. The energy spectrum of primary protons incident on the upper boundary of the atmosphere obeys approximately the following empirical law: $N(T) = K/(1 + T)$. Here, T (GeV) is the kinetic energy, $N(T)$ is the number of protons per cm²·sec·ster (the directional intensity) with an energy higher than T , and $K = 0.38$. In the current study, the energy spectrum of primary radiation was ascertained using this formula and was specified in the energy interval from 100 MeV to 10 GeV. Protons of such energies enter the atmosphere near the geomagnetic poles. According to [15], it can be shown that the total flux of protons from all directions at the boundary of the atmosphere is equal to the directional intensity multiplied by π . The energy spectrum of the protons and the intensity were selected such that the total primary flux at each latitude is in agreement with the data [16]. In conformity with this spectrum, on the average about 2.8 protons per cm²·sec with an energy lying between 0.1 and 10 GeV enter the atmosphere. This corresponds to an energy density of 2.89 GeV/(cm²·sec), or a mean energy of 3.35 GeV per proton.

Passage of the nucleonic component was modeled with allowance for the variation in the atmospheric density with the altitude. The composition of the atmosphere and the mass fractions of its constituents (N₂, O₂, Ar, N, O, He, and H) were calculated on the basis of the MSISE-90 empirical model of the neutral atmosphere [17], including CIRA-86 data [18]. Since collisions of protons with nuclei of air atoms occur starting of 90 km, consideration was given only to the part of the atmosphere from an altitude of 90 km and lower.

Passage of the nucleonic component was studied in a plane geometry. An altitude of 90 km was taken as the zero reference point. The entire atmospheric region considered was broken up into 900 layers with a different step. At the earth's surface, the step was reduced so that the air density within each layer could be assumed to be constant. Part of the secondary radiation of the nucleonic component reaches the earth's surface and penetrates into the soil. Therefore, a soil thickness of 20 m was examined. It was split into 200 layers with a constant step. The average density of the soil was taken to be 2.75 g/cm³. The mass content of the main chemical elements of the soil employed in the calculation was taken from the reference book [19].

Figure 1a shows the height distribution of the rate of ion formation created by cosmic radiation in the atmosphere. It is seen from this figure that the rate of ion formation increases with the atmospheric depth approximately linearly. Figure 1b presents a profile of the ion-formation rate as a function of the depth of the earth's crust. It ensues from the figure that at the air-soil boundary a jump in the rate of ion-electron pair formation by about three orders of magnitude occurs. For the soil composition employed, the rate of ion formation

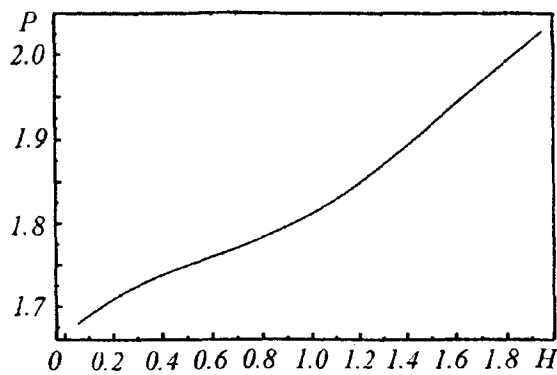


Fig. 2. Power of the absorbed dose of ionizing radiation near the earth's surface. P , rad/yr.

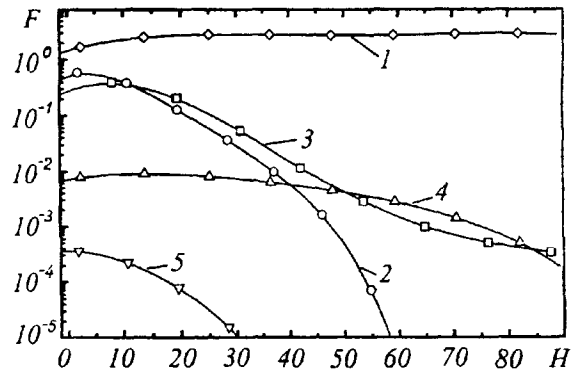


Fig. 3. Distribution of particle fluxes over the atmospheric height: 1) protons; 2) neutrons; 3) photons; 4) electrons; 5) positrons. F , particle/($\text{cm}^2 \cdot \text{sec}$).

decreases to the value near the earth's surface (Fig. 1b) at a depth of about 20 m. Figure 2 illustrates the distribution of the yearly dose absorbed in the air near the earth's surface. If it is necessary to calculate the dose power not in the air but rather in some absorbing medium, mass scaling factors [20] can be used. Here it should be noted that the calculated rate of ion formation in the atmosphere and in the earth's crust and the power of the dose of absorbed radiation near the earth's surface are overestimated (by about 50 times) because the creation of π -mesons in nuclear interactions was disregarded. In the nuclear collisions discussed thus far, each elementary event inside a nucleus was an elastic interaction between an incident nucleon and one of the intranuclear nucleons. However, a high-energy (> 400 MeV) nucleon is also very likely to experience an inelastic collision with one of the intranuclear nucleons. In this case, a significant portion of the kinetic energy of the incident nucleon is spent on forming one or more charged or neutral π -mesons. The threshold for meson formation is determined by the rest energy $m_{\pi}c^2 \approx 141$ MeV and the laws of conservation of energy and momentum. Therefore, as a minimum the energy $m_{\pi}c^2$ is spent on forming a single meson. As a result of the creation of π mesons, part of the energy of the nucleonic component is transferred to other (electron-photon and μ -meson) components emerging in the upper part of the atmosphere, and active nuclear particles near the earth's surface turn out to be much fewer in number. Hence, the density of ionic pairs formed by cosmic rays at the level of the earth's surface and the power of the dose absorbed in the air will be appreciably lower.

Figure 3 presents the distribution of particle fluxes formed as the nucleonic component passes as a function of the atmospheric height. The neutron flux originates at a height below 60 km and increases with the atmospheric depth due to direct nuclear reactions and evaporation of residual nuclei. The electron flux is related to ionization of atmospheric atoms by protons and charged particles emitted from nuclei. The photon flux arises from bremsstrahlung radiation of electrons and de-excitation of residual nuclei. Since electrons and photons cannot have a significant energy as a result of these processes, bremsstrahlung radiation and the creation of electron-positron pairs do not play an important role and cannot give rise to the electron-photon component. For the appearance of the electron-photon and muonic cascades observed in the atmosphere, account should be taken of the formation of π -mesons in nuclear collisions in the present theoretical model.

Consideration was also given to the energy and angular spectra of protons, neutrons, photons, and electrons formed as a nucleonic-nuclear cascade traverses the atmosphere. These spectra permit determination of the average number of the above-stated particles in specified ranges of energies and angles at certain heights. As a result of the investigation, the energy spectrum of protons was found to extend up to energies of 10 GeV, since protons are particles incident on the upper boundary of the atmosphere. Closer to the earth's surface (~ 2 km) a low-energy part of the spectrum associated with secondary protons knocked out and evaporated from nuclei appears. Also, angular broadening of the proton flux with increase in the atmospheric depth occurs. Neutrons emerge from direct reactions of nucleons with nuclei, and their energy spectrum reaches an energy of the order of 2 GeV. A significant portion of the neutrons derives from evaporation of residual nuclei, and therefore the maximum of the energy

spectrum is about 8 MeV. The energy spectrum of photons is confined to the interval of 10 keV–10 MeV. Electrons originate due to ionization of atmospheric atoms by protons and cannot have a significant energy either. The distributions presented are obtained as a result of 11,220 traced histories of primary protons with an energy ascertained from the energy spectrum.

The cutoff energy for electrons and positrons was taken to be 100 keV, and for protons, 500 keV. After this energy was attained, charged particles were assumed to be absorbed. Secondary particles with energies lower than the cutoff energy were not considered either. The cutoff energy for photons and neutrons was taken to be 1 keV. This choice of values is stipulated by the fact that the mean free path of these particles with an energy lower than the cutoff energy is not larger than the cell size. The mean percentage of secondary particles emerging in the energy ranges considered is about 64.1% electrons, 16.8% ions, 13.5% photons, 5% neutrons, and 0.6% positrons per primary proton.

Conclusion. The developed theoretical models and the created program complexes permit a description of the passage of electron-photon [14] and nucleonic-nuclear cascades individually through the earth's atmosphere. The creation of charged and neutral π -mesons in inelastic nuclear collisions is the link between these components of cosmic radiation and also the μ -component. Neutral π -mesons break down into two high-energy photons, which form an electron-photon cascade. Charged π -mesons break down into μ -mesons and a neutrino and give rise to a μ -component. Thus, π -mesons can be regarded as the link between the primary nucleonic and the secondary electron-photon and μ -components. Therefore, further investigation should aim at working out a theoretical model that describes the formation and interaction of π -mesons and establishes a genetic connection between the components of cosmic radiation. For this it is necessary to determine the total and differential cross sections of interaction of π -mesons with nucleons and atmospheric nuclei based on solving numerically the relativistic Klein–Gordon equation [21].

The work was carried out with support of the International Science and Technology Center, project B23-96.

NOTATION

θ , scattering angle of the particle; θ^* , angle separating weak and strong scattering; L , trajectory length between two successive collisions; ΔT , energy transfer as a result of the collision; T^* , energy separating distant and near collisions; σ_t , total microscopic cross section; σ_s , total cross section of elastic scattering; σ_r , microscopic cross section of the reactions; k , wave number of the nucleon; l , orbital quantum number; $S_{l\pm 1/2}$, elements of the scattering matrix; Ω , solid angle of scattering; Y_l , normalized spherical functions; T , kinetic energy of the incident particle; T_F , Fermi energy; T_N , kinetic energy of a secondary nucleon; ϵ , binding energy of the nucleon in the nucleus; T_b , cutoff energy; E^* , excitation energy of the residual nucleus; E , overall kinetic energy of particles emitted from the nucleus; W , binding energy of the parent nucleus; U , binding energy of the residual nucleus after passage of the intranuclear cascade; m_π , mass of a π -meson; c , speed of light; H , atmospheric height; D , depth of radiation penetration; F , particle fluxes. Subscripts: t, total cross section; s, elastic scattering; r, nuclear reaction; l, orbital number; b, boundary energy.

REFERENCES

1. B. B. Kadomtsev, *Zh. Éksp. Teor. Fiz.*, **33**, Issue 1, 151-157 (1957).
2. V. B. Berestetskii, E. M. Lifshits, and L. P. Pitaevskii, *Quantum Electrodynamics* [in Russian], Moscow (1980).
3. I. B. Marion and B. A. Zimmerman, *Nucl. Instrum. Methods*, **51**, 93-97 (1967).
4. Yu. V. Gott, *Interaction of Particles with Matter in Plasma Studies* [Russian translation], Moscow (1978).
5. H. Feshbach, C. E. Porter, and V. F. Weisskopf, *Phys. Rev.*, **96**, 448-464 (1954).
6. P. E. Hodgson, *Optical Model of Elastic Scattering* [Russian translation], Moscow (1966).
7. G. I. Marchuk and V. E. Kolesov, *Use of Numerical Methods for Calculating Neutron Cross Sections* [in Russian], Moscow (1970).
8. V. S. Barashenkov and V. D. Toneev, *Interactions of High-Energy Particles and Atomic Nuclei with Nuclei* [in Russian], Moscow (1972).

9. I. M. Sobol', *Monte Carlo Numerical Methods* [in Russian], Moscow (1973).
10. E. Hara, *Nucl. Instrum. Methods*, **65**, 85-92 (1968).
11. A. M. Kol'chuzhkin and V. V. Uchaikin, *Introduction to the Theory of Passage of Particles through Matter* [in Russian], Moscow (1978).
12. G. Bernardini, E. T. Booth, and S. Lindenbaum, *Phys. Rev.*, **88**, 1017-1026 (1952).
13. B. N. Belyaev and I. V. Tsaritsyna, *Computational Methods (Collection of Papers)*, No. 1, 76-107 (1963).
14. G. V. Miloshevskii, *Monte Carlo Model for Numerical Simulation of Combined Photon-Electron Transport in Composite Targets*, Preprint of the Academic Scientific Complex "A. V. Luikov Heat and Mass Transfer Institute," National Academy of Sciences of Belarus [in Russian], Minsk (1997).
15. B. Rossi, *Cosmic Rays* [Russian translation], Moscow (1966).
16. B. Rossi, *High-Energy Particles* [Russian translation], Moscow (1955).
17. A. E. Hedin, *J. Geophys. Res.*, **96**, 1159-1167 (1991).
18. D. Rees (ed.), *Advances in Space Research*, **8**, Nos. 5-6 (1988).
19. I. S. Grigor'ev and E. Z. Meilikhov (eds.), *Physical Quantities: Manual* [in Russian], Moscow (1991).
20. V. A. Budarkov, V. A. Kirshin, and A. F. Antonenko, *Radiobiological Manual* [in Russian], Minsk (1992).
21. H. Bethe, *Quantum Mechanics* [Russian translation], Moscow (1965).